

PlaceRAN: Optimal Placement of Virtualized Network Functions in the Next-generation Radio Access Networks

Fernando Zanferrari Moraes, Gabriel Matheus F. de Almeida, Leizer Pinto, Kleber Vieira Cardoso, Luis M. Contreras, Rodrigo da Rosa Righi, and Cristiano Bonato Both



Abstract—The fifth-generation mobile evolution introduces Next-Generation Radio Access Networks (NG-RAN), splitting the RAN protocol stack into the eight disaggregated options combined into three network units, i.e., Central, Distributed, and Radio. NG-RAN enables the management of network units and the protocols disaggregated as radio functions. These functions' placement is challenging since the best decision is based on the RAN protocol stack split, routing paths of transport networks with restricted bandwidth and latency requirements, different topologies and link capabilities, asymmetric computational resources, etc. This article proposes the first exact model for the placement optimization of radio functions for NG-RAN planning, named PlaceRAN. The main objective is to minimize the computing resources and maximize the aggregation of radio functions. The PlaceRAN evaluation considered two real network topologies based on 5G-crosshaul and Passion European projects. Our results show that the PlaceRAN model achieves an optimal high-performance aggregation level. Moreover, we prove that PlaceRAN is flexible for RAN deployment overcoming the network restrictions. Therefore, PlaceRAN is the most innovative approach to provide advanced NG-RAN design and development.

Index Terms—Placement optimization, vNG-RAN, Disaggregation

1 INTRODUCTION

THE fifth-generation mobile evolution is based on standards [1]–[3] defining the virtualization of the Radio Access Network (vRAN) on the protocol stack disaggregation and the software-based networking. These standards specify the Next Generation RAN (NG-RAN) architecture to meet the new network demands, e.g., ultra-low latency and high-bandwidth applications. Furthermore, the industry creates its initiatives for NG-RAN. The most promising are based on open solutions, called Open RAN (O-RAN), focused on general-purpose vendor-neutral hardware, software-defined technologies, and interoperability [4]. The NG-RAN architecture proposed enables the base station for splitting the protocol stack into the eight options combined into three network elements: (i) Central Unit

(CU), (ii) Distributed Unit (DU), and (iii) Radio Unit (RU) [2], [5]. These split options concern improving the radio functions and cost efficiency compared with the last mobile generations [5], [6].

The network software process in NG-RAN is guided by the virtualization of nodes and radio functions by the Network Function Virtualization (NFV) concept [7], [8]. For example, the NG-RAN architecture functional split combined with vRAN provides flexibility for mobile access networks. This flexibility allows mobile network operators to place the radio functions to take into account available network resources and user demand. The placement of radio functions in a fine-grained network management approach is considered vital for fifth-generation networks to achieve the expected leadership of digital transformation. However, the development of the virtualized NG-RAN architecture (vNG-RAN) is an unprecedented challenging problem since crosshaul transport networks (backhaul, midhaul, and fronthaul) have restricted bandwidth and latency requirements, different topologies and link capabilities, asymmetric computing resources (CR), and unbalanced user demand [2], [9].

vNG-RAN is up-to-date in fifth-generation research, although no decision-making method for specification designing of the placement of virtualized radio network functions is defined. The placement is defined on the optimization problem [10], [11] based on the best joint decision between the split of the RAN protocol stack, the routing paths of the crosshaul network, and the CRs strategies of the CU, DU, and RU nodes [11]. Therefore, the ideal placement leads to analysis related to the bandwidth and latency requirements for each split option between CU-DU and DU-RU. Moreover, each split option results in a computing cost (processing, memory, and storage) to be evaluated. According to the network's scalability, the placement needs to be aware of the load occupation, even routing and computing resources allocation.

In the literature, several works lead to the placement optimization of radio functions. The main strategies developed are to maximize the number of VNFs running in a single CU, DUs fixes, and close to RUs [12], [13]. Moreover, CU is co-located with the core [14]. The state-of-the-art is restricted considering the protocol disaggregations number, reaching

- Fernando Zanferrari Moraes, Rodrigo da Rosa Righi, and Cristiano Bonato Both are with the University of Vale do Rio dos Sinos (UNISINOS).
- Gabriel Matheus, Leizer Pinto, Kleber Vieira Cardoso are with the Universidade Federal de Goiás (UFG).
- Luis M. Contreras is with the Transport & IP Networks - Systems and Network Global Direction, Telefónica GCTIO Unit.

the maximum of five [15], efficiency under crosshaul constraints (mainly, the fronthaul network) [12], [16], [17], and computing resources [18], [19]. Therefore, to the best of our knowledge, no work in the literature considers CUs, DUs, and RUs for real-world networks, making the problem more general with high functional split options and protocol stack analysis.

Contributions. In this article, we introduce PlaceRAN, the problem formulation for the optimal placement of vNG-RAN functions. The problem is formulated as the best trade-off between maximizing the aggregation level of virtualized NG-RAN functions and minimizing the number of computing resources necessary for running these functions. PlaceRAN innovates by considering in the formulation all RAN elements (CU, DU, and RU), the paths between these elements (fronthaul, midhaul, and backhaul), and also all functional splits according to the standards. Our contributions can be summarized as follows:

- **New problem formulation** – in some aspects, PlaceRAN is the most general problem formulation in the context of vNG-RAN, and it was designed with a comprehensive set of real-world NG-RANs considerations in mind.
- **New approach** – we introduced some concepts to properly formulate PlaceRAN, such as Disaggregated RAN Combination (DRC) and multi-stage problem formulation, turning the problem formulation simple despite its generality.
- **Efficient exact solution** – we solve PlaceRAN using a conventional solver (i.e., IBM CPLEX) for real-world RAN instances despite the problem complexity.
- **Evaluation and new insights** – our evaluation employed examples of present and future RANs. We show how PlaceRAN contributes to deal with the optimal placement of forthcoming vNG-RANs.
- **Relevant results** – the results show that PlaceRAN offers the necessary flexibility to overcome the network constraints, achieving the high aggregation levels up to two centralized nodes near the core.

Article organization. Section 2 introduces the vNG-RAN background. The PlaceRAN system model and problem statement are described in Section 3. Section 4 presents the PlaceRAN evaluation methodology and results. The related work is discussed in Section 5, and finally, Section 6 presents the final remarks.

2 VIRTUALIZED NG-RAN PLACEMENT

The fundamental idea of a disaggregated NG-RAN is to decompose the RAN functions into virtualized components that can be distributed to run into different computing devices, i.e., a non-monolithic approach. Therefore, it is necessary to identify how this decomposition can be performed and which conditions must be satisfied to have the disaggregated version running correctly. This disaggregated NG-RAN is defined by the concept of *functional splits* that specifies all the network functions, clear interface points between them, and the requirements of each network function [4], [20].

TABLE 1
3GPP Latency and bitrate requirements for each split.

Split Option	Functional Split	One-way latency	Bitrate (Gbps)	
			DL	UL
O1	RRC-PDCP	10 ms	4	3
O2	PDCP - High RLC	10 ms	4	3
O3	High RLC - Low RLC	10 ms	4	3
O4	Low RLC - High MAC	1 ms	4	3
O5	High MAC - Low MAC	< 1 ms	4	3
O6	Low MAC - High PHY	250 μ s	4.13	5.64
O7	High PHY - Low PHY	250 μ s	86.1*	86.1*
O8	Low PHY - RF	250 μ s	157.3	157.3

O7 split maximum value.*

The number of functional splits and where they occur are determined by specifications from standardization bodies, such as Release 14 from 3GPP [21] and IMT-2020/5G from ITU-T [2]. Table 1 shows the specifications of the disaggregated protocol stack employed in this work. The (maximum) latency and (minimum) bitrate values must be satisfied with the communication of the RAN nodes (CU, DU, and RU) even if they are running on different computing devices. The latency and bitrate must be assured according to the functional split specified. The (maximum) latency and (minimum) bitrate values presented in the table correspond to an RU with the following configuration: 100 MHz bandwidth, 32 antenna ports, 8 MIMO layers, and 256 QAM modulation [21].

Each RAN node (CU, DU, and RU) is considered a network function virtualized as part of a disaggregated NG-RAN (3 independent nodes) composed of RAN protocols embedded in Virtualized Network Functions (VNFs). Moreover, each RAN node may be identified by the set of all RAN protocols running into it, as shown in Fig. 1. A configuration with less than three nodes may be named as DU and RU integration (DU and RU), C-RAN (CU and DU), or D-RAN (CU, DU, and RU) [2]. In a disaggregated NG-RAN, the paths along the network connecting the core to vCU, vCU to vDU, and vDU to RU are defined as backhaul, midhaul, and fronthaul, respectively. This terminology is useful since each physical link of the access network acts as a crosshaul, meaning that it can transport any combination of the previous paths. The crosshaul needs to ensure the latency and bitrate required according to the functional splits [9], [20].

As illustrated in Fig. 1, each functional split and the corresponding placement of VNFs in a specific RAN node characterize a *Disaggregated RAN Combination* (DRC). The concept of DRC, introduced in this article, represents the preservation of the protocol stack order during the processing of the VNFs. Nineteen DRCs are mapped considering seven split options. The O8 option is not virtualized since the RF protocol is hardware-based, making virtualization impractical. Certain DRCs are not used in practice because they are not cost-effective, e.g., midhaul with less than 1 ms, or they lack advantages in the RAN disaggregation.

We highlighted the nine DRCs effectively adopted in vRAN deployments, whose choice is based on standardization bodies and industry alliances [1]–[3]. In both architectures of three independent nodes (O-RAN and Smallcell Forum), the focus is on O1 and O2 (Fig. 1 - DRC1, DRC2,

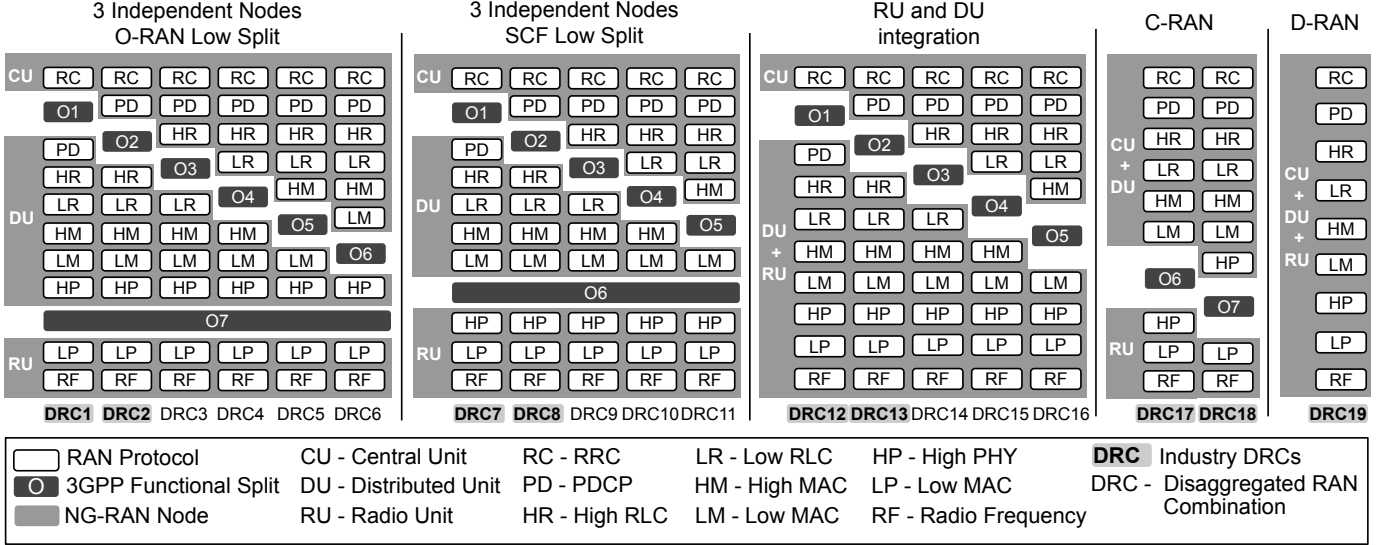


Fig. 1. Functional split and computing devices for a disaggregated NG-RAN.

DRC7, and DRC8). The industry considers split O1 as a possibility of the decentralized data plane. Split O2 is consolidated by 3GPP and ITU-T via the F1 interface and is an industry reference for O-RAN and Smallcell Forum initiatives [2], [22], [23]. Two industry DRCs were chosen for the DU and RU integration (Fig. 1 - DRC12 and DRC13), besides of the two C-RAN options (Fig. 1 - DRC17 and DRC18). These splits align with ITU-T (mainly due to crosshaul constraints) and O-RAN and Smallcell Forum initiatives [4], [22]. Naturally, the traditional D-RAN architecture is also supported to provide scenarios where the crosshaul is very limited [2] (Fig. 1 - DRC19).

In summary, the disaggregated NG-RAN can be implemented as a virtual network service, i.e., a collection of VNFs with a particular set of characteristics. First, the service consists of process one protocol stack per RF device in NG-RAN. This processing implies an appropriate order of the flow-through VNFs, i.e., Service Function Chain (SFC) to be respected. VNFs are instantiated in the RAN nodes, which are also virtual elements that can run in different computing devices in NG-RAN. The choice of where to position the RAN nodes and their VNFs affects the resources applied, including computing and networking. For each NG-RAN topology and set of resources, there may be multiple options for positioning VNFs and RAN nodes. In general, the objective is to consume the minimum resources and group the maximum of VNFs related to the same protocol or layer. However, each positioning option implies different computing and networking demands, which must not exceed the available resources. Therefore, the function's placement becomes a complex optimization problem that we will formally present in the next section.

3 MODEL AND PROBLEM STATEMENT

Initially, Subsection 3.1 presents the system model of a virtualized formally and disaggregated NG-RAN, in which different functional splits are possible. Moreover, the placement of the virtual functions also is introduced with multi-

ple options. Second, Subsection 3.2 formulates the optimization problem of jointly minimizing the number of necessary computing resources, selecting the functional splits, and placing the virtual functions.

3.1 System Model

Nodes and links. According to the 3GPP standards (Release 15 [1] and Release 16 [24]), we consider RAN of a mobile network connection to the core network, as illustrated by Fig. 2. RAN is composed of:

- A set $\mathcal{B} = \{b_1, b_2, \dots, b_{|\mathcal{B}|}\}$ of RUs, i.e., nodes hosting the Low PHY sublayer and the RF processing based on a lower layer functional split.
- A set $\mathcal{C} = \{c_1, c_2, \dots, c_{|\mathcal{C}|}\}$ of CRs that may process the virtual functions. Each CR c_m has a processing capacity c_m^{Proc} (given in some reference cores). Moreover, each CR has other characteristics, such as memory and storage capacity, but they are not commonly exhausted before the processing capacity in the context of disaggregated RAN. A CR may connect directly to an RU.
- A set $\mathcal{T} = \{t_1, t_2, \dots, t_{|\mathcal{T}|}\}$ of transport nodes, which may connect to RUs, CRs, core, or each other.

To represent RAN and core, we define the graph $G = (\mathcal{V}, \mathcal{E})$, with $\mathcal{V} = \{v_0\} \cup \mathcal{B} \cup \mathcal{C} \cup \mathcal{T}$ being the set of nodes and $\mathcal{E} = \{e_{ij}; v_i, v_j \in \mathcal{V}\}$, $v_i, v_j \in \mathcal{V}$ representing the set of network links connecting the nodes. v_0 represents the core and it is the source/destination for all flows. Each link $e_{ij} \in \mathcal{E}$ has a transmitting capacity e_{ij}^{Cap} (given in multiples of bps) and a latency e_{ij}^{Lat} (given in fractions of a second).

Paths and routing. We consider that all network traffic has the core as its source (downlink) or destination (uplink). However, without loss of generality, we represent only the downlink case in this work. We define \mathcal{P}_l as the set of k -shortest paths from the core to each RU $b_l \in \mathcal{B}$. Each path $p \in \mathcal{P}_l$ is composed of three sub-paths: p_{BH} (backhaul),

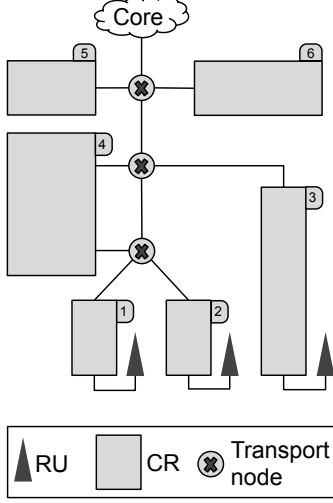


Fig. 2. RAN considered as a reference to the system model.

p_{MH} (midhaul), and p_{FH} (fronthaul), in which at least one of these sub-paths is not empty.

Virtualized RAN functions. We consider that a VNF runs a protocol of RAN stack (except the RF protocol, as detailed previously). Moreover, VNFs are labeled in increasing order, starting from PHY Low with f_1 and ending at RRC with f_8 . We define $\mathcal{F} = \{f_1, f_2, f_3, f_4, f_5, f_6, f_7, f_8\}$ as the set of disaggregated RAN VNFs, where the distribution must follow one of the industry DRCs [2], [23] of the set $\mathcal{D} = \{D_1, D_2, \dots, D_{|\mathcal{D}|}\}$ (illustrated in Fig. 1).

3.2 PlaceRAN Problem Formulation

Our problem has two objectives: (i) maximize the aggregation level of RAN VNFs and (ii) minimize the number of CRs used for this aggregation. Since the computing and network capacities are limited, decreasing the number of CRs may not imply an increase in the aggregation level, which creates conflicting objectives. However, there is a clear relationship between the number of CRs and the aggregation level. Additionally, the functional splits' aggregation level is not measured only by the number of VNFs and CRs. The aggregation level is also affected by two other metrics: the number of DRCs employed and the priority or preference of each DRC. Since three incompatible metrics measure the aggregation level, we designed our formulation into three stages. The optimal solution can be eventually obtained in the first or second stage, but we are sure about it only in the third stage, after resolving all potential draws.

First Stage

In the first stage, the objective is jointly to maximize the number of grouped RAN VNFs and minimize the number of CRs used to run these VNFs. We define $x_l^{p,r} \in \{0, 1\}$ as the decision variable representing which path $p \in \mathcal{P}_l$ and DRC $D_r \in \mathcal{D}$ is selected to serve RU $b_l \in \mathcal{B}$. From the input data, we determine $u_m^p \in \{0, 1\}$ to indicate if $c_m \in \mathcal{C}$ is part of the $p \in \mathcal{P}_l$. Additionally, we define the mapping function $M(c_m, f_s, b_l, D_r) \in \{0, 1\}$ over the input data, which indicates if the CR $c_m \in \mathcal{C}$ runs the VNF $f_s \in \mathcal{F}$ from

the RU $b_l \in \mathcal{B}$, according to the DRC $D_r \in \mathcal{D}$. Therefore, we define the following objective function:

$$\text{minimize } \Phi_1 - \Phi_2, \quad (1)$$

where Φ_1 represents the amount of CRs, given by:

$$\Phi_1 = \sum_{c_m \in \mathcal{C}} \left[\frac{\sum_{b_l \in \mathcal{B}} \sum_{D_r \in \mathcal{D}} \sum_{p \in \mathcal{P}_l} (x_l^{p,r} \cdot u_m^p)}{|\mathcal{C}|} \right], \quad (2)$$

and Φ_2 represents the amount of grouped RAN VNFs, given by:

$$\Phi_2 = \sum_{c_m \in \mathcal{C}} \sum_{f_s \in \mathcal{F}} \left(\frac{\sum_{b_l \in \mathcal{B}} \sum_{D_r \in \mathcal{D}} \sum_{p \in \mathcal{P}_l} [x_l^{p,r} \cdot u_m^p \cdot M(c_m, f_s, b_l, D_r)]}{\left| \frac{\sum_{D_r \in \mathcal{D}} \sum_{p \in \mathcal{P}_l} \sum_{b_l \in \mathcal{B}} [x_l^{p,r} \cdot u_m^p \cdot M(c_m, f_s, b_l, D_r)]}{|\mathcal{F}|} \right|} \right). \quad (3)$$

For each RU $b_l \in \mathcal{B}$, exactly one DRC $D_r \in \mathcal{D}$, using a single path $p \in \mathcal{P}_l$, must be selected, as represented by the following constraint:

$$\sum_{D_r \in \mathcal{D}} \sum_{p \in \mathcal{P}_l} x_l^{p,r} = 1, \quad \forall b_l \in \mathcal{B}. \quad (4)$$

The transmitting capacity e_{ij}^{Cap} of every link e_{ij} must not be exceeded, as described by the following constraint:

$$\sum_{b_l \in \mathcal{B}} \sum_{D_r \in \mathcal{D}} \sum_{p \in \mathcal{P}_l} \left[x_l^{p,r} \left(y_{e_{ij}}^{p,BH} \cdot \alpha_{BH}^r + y_{e_{ij}}^{p,MH} \cdot \alpha_{MH}^r + y_{e_{ij}}^{p,FH} \cdot \alpha_{FH}^r \right) \right] \leq e_{ij}^{Cap}, \forall e_{ij} \in \mathcal{E}, \quad (5)$$

where $y_{e_{ij}}^{p,BH}$, $y_{e_{ij}}^{p,MH}$, and $y_{e_{ij}}^{p,FH}$ indicate if the link e_{ij} is part of the backhaul, midhaul, or fronthaul, respectively, in a path $p \in \mathcal{P}_l$ that transports a specific DRC $D_r \in \mathcal{D}$. Each $D_r \in \mathcal{D}$ has associated demands for bitrate in the backhaul, midhaul, and fronthaul, represented by α_{BH}^r , α_{MH}^r , and α_{FH}^r , respectively. There are functional splits in which the path $p \in \mathcal{P}_l$ has less than three sub-paths, e.g., DRCs 12, 17, and 19 (as illustrated in Fig. 1). Moreover, if the sub-path is absent, then no link is part of it.

Each $D_r \in \mathcal{D}$ tolerates a maximum latency in each sub-path (backhaul, midhaul, and fronthaul) of the path $p \in \mathcal{P}_l$, which is described by the following constraints:

$$\sum_{e_{ij} \in \mathcal{E}} x_l^{p,r} \cdot y_{e_{ij}}^{p,BH} \cdot e_{ij}^{Lat} \leq \beta_{BH}^r, \forall b_l \in \mathcal{B}, p \in \mathcal{P}_l, D_r \in \mathcal{D}, \quad (6)$$

$$\sum_{e_{ij} \in \mathcal{E}} x_l^{p,r} \cdot y_{e_{ij}}^{p,MH} \cdot e_{ij}^{Lat} \leq \beta_{MH}^r, \forall b_l \in \mathcal{B}, p \in \mathcal{P}_l, D_r \in \mathcal{D}, \quad (7)$$

$$\sum_{e_{ij} \in \mathcal{E}} x_l^{p,r} \cdot y_{e_{ij}}^{p,FH} \cdot e_{ij}^{Lat} \leq \beta_{FH}^r, \forall b_l \in \mathcal{B}, p \in \mathcal{P}_l, D_r \in \mathcal{D}, \quad (8)$$

where β_{BH}^r , β_{MH}^r , and β_{FH}^r represent the maximum latency tolerated in the backhaul, midhaul, and fronthaul, respectively, of a path $p \in \mathcal{P}_l$ that transports a specific DRC $D_r \in \mathcal{D}$. There are functional splits in which the path $p \in \mathcal{P}_l$ has less than three sub-paths. In the same way, if the sub-path is absent, then no link is part of it.

Finally, the VNFs selected to run in a CR $c_m \in \mathcal{C}$ must not exceed its processing capacity c_m^{Proc} , as represented by the following constraint:

$$\sum_{f_s \in \mathcal{F}} \sum_{b_l \in \mathcal{B}} \sum_{D_r \in \mathcal{D}} \sum_{p \in \mathcal{P}_l} x_l^{p,r} \cdot u_m^p \cdot M(c_m, f_s, b_l, D_r) \cdot \gamma_m^s \leq c_m^{Proc}, \quad \forall c_m \in \mathcal{C}, \quad (9)$$

where γ_m^s is the computing demand of the VNF $f_s \in \mathcal{F}$.

Second Stage

After solving the first stage, we obtain the minimum number of CRs necessary to achieve the maximum aggregation level of RAN VNFs. Since these two objectives may be conflicting, the first stage's final result is the best trade-off between these goals. However, the aggregation level achieved may not be optimal. An example is illustrated in Fig. 3, where solution 1A and solution 1B are two possible solvers' outcomes. In this case, both solutions have the same value of object function, i.e., both achieve the same value for Equation (1).

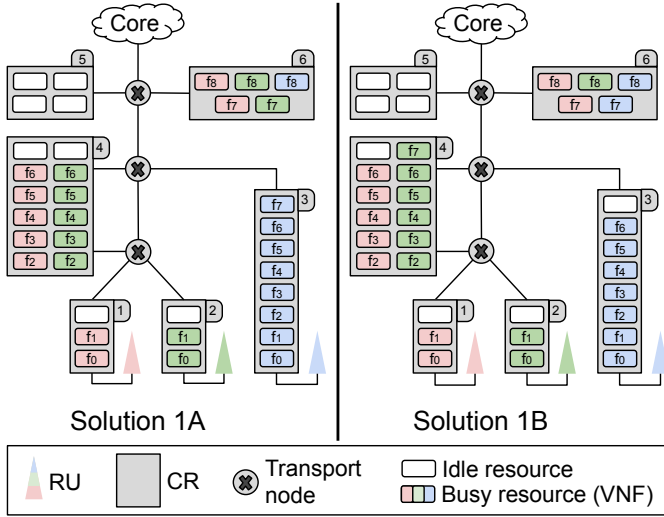


Fig. 3. A possible tie after solving the first stage.

While comparing different solutions with the same value for the objective function (Equation (1)) in the first stage, we observed that those with a smaller number of DRCs combine, sharing the same virtualized RAN function \mathcal{F} and CR, improving the system performance. For example, in Fig. 3, there is a benefit in sharing CR 6 by f_7 (PDCP) from the red flow and f_7 from the green flow (solution 1A). However, there is no benefit in sharing CR 6 by f_7 (PDCP) from the red flow and f_7 from the blue flow (solution 1B). Solution 1A has two DRCs: 2 and 12, while solution 1B has three DRCs: 1, 2, and 13. Therefore, the objective function of the second stage is to minimize the number of DRCs:

$$\text{minimize} \quad \sum_{D_r \in \mathcal{D}} \left\lceil \frac{\sum_{b_l \in \mathcal{B}} \sum_{p \in \mathcal{P}_l} x_l^{p,r}}{|\mathcal{B}|} \right\rceil. \quad (10)$$

This second stage must consider only solutions with exactly the same value of the objective function achieved by the optimal solution from the first stage. The following constraint assures this situation:

$$\Phi_1 - \Phi_2 = f_{1st_stage}(x_l^{p,r*}), \quad (11)$$

where $f_{1st_stage}(x_l^{p,r*})$ represents the objective function's value from the first stage when the optimal solution is found. Additionally, all constraints from the first stage must also be satisfied, i.e., the second stage is subject to the constraints (4)–(9).

Third Stage

After solving the second stage, we eliminate potential solutions that have incompatible layers sharing common CRs. While this improves the aggregation level, there is still the possibility of obtaining different solutions with the same number of DRCs, but not equivalent. An example is illustrated in Fig. 4, where solution 2A and solution 2B are two possible solvers' outcomes. These solutions have the same value of object function, i.e., both achieve the same value for Equation (10). In this case, solution 2A has two DRCs: 2 and 12, while solution 2B also has two DRCs: 1 and 12.

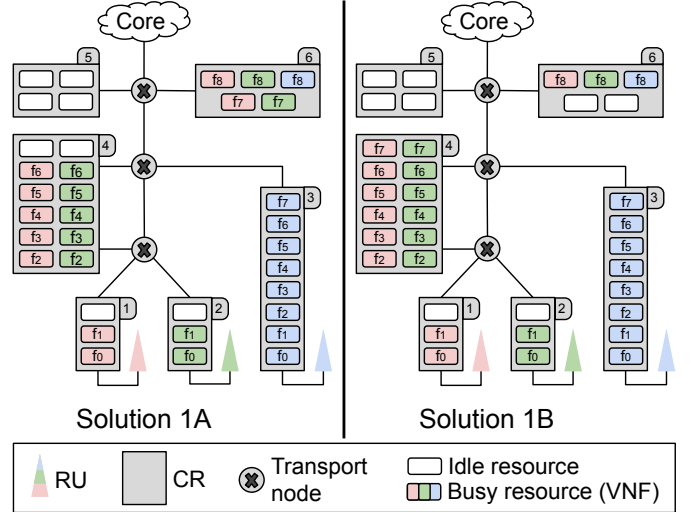


Fig. 4. A possible tie after solving the second stage.

The solutions in Fig. 4 are not equivalent because each DRC has characteristics that make it unique, i.e., it is possible to rank DRCs and the solution's quality. By ranking DRCs, we are also able to differentiate the solutions again. This rank can be directly extracted from the standards, which already specify the preference order of DRCs. Naturally, different standardization bodies (e.g., O-RAN and ITU) may assign other priorities to DRCs, but our model is generic and works properly with any of them. In the priority assignment for each DRC, the smaller the value, the higher priority. Therefore, the objective function of the third stage is to minimize the sum of values assigned to DRCs:

$$\text{minimize} \quad \sum_{b_l \in \mathcal{B}} \sum_{D_r \in \mathcal{D}} \sum_{p \in \mathcal{P}_l} (x_l^{p,r} \cdot D_r^\omega), \quad (12)$$

where D_r^ω represents the priority of the DRC D_r .

The third stage must also consider only solutions with exactly the same value of the objective function achieved by the optimal solution from the first stage, i.e., the constraint described by Equation 11 and the exact value of the objective function given by the second stage's optimal solution. The following constraint assures this definition:

$$\sum_{D_r \in \mathcal{D}} \left[\frac{\sum_{b_l \in \mathcal{B}} \sum_{p \in \mathcal{P}_l} x_l^{p,r}}{|\mathcal{B}|} \right] = f_{2nd_stage}(x_l^{p,r*}), \quad (13)$$

where $f_{2nd_stage}(x_l^{p,r*})$ represents the value of the objective function from the second stage when the optimal solution is found. Similarly to the second stage, all constraints from the first stage must also be satisfied, i.e., the third stage is subject to the constraints (4)–(9).

4 EVALUATION

This section evaluates the PlaceRAN model in several RAN configurations, including T1 present and T2 future network topologies, different amounts of resources, and distinct demands. Subsection 4.1 provides a general description of the evaluated scenarios, detailing the topologies, resources, and which parameters are varied to assess the solution results. Subsection 4.2 presents and discusses the results obtained in the evaluation of PlaceRAN, which involves DRC selection, minimization of CRs versus maximization aggregations level, general aspects of the solutions, and characteristics of the optimization model.

4.1 Description of the Scenarios

Table 2 summarizes the scenarios employed in the evaluation of the PlaceRAN model. There are three types of scenarios: Low Capacity (LC), Random Capacity (RC), and High Capacity (HC). Each scenario has four types of Transport Nodes, which are defined according to the proximity to the Core and the number of neighbors: aggregation node 1 (AG1), aggregation node 2 (AG2), access node 1 (AC1), and access node 2 (AC2). Based on each transport node, there are four characteristics of real networks: (i) number of CRs, (ii) Bandwidth, (iii) Latency, and (iv) number of RU nodes. Moreover, our evaluation is focused on comparing the scenarios and two topologies. T1 represents the current RANs and based on the 5G-crosshaul project (in Table 2 as †). T2 shows a trend in the design of the future RANs and aligned with the PASSION project (in Table 2 as ‡).

Transport Nodes. We associate the nodes according to T1 and T2 topologies. T1 provides a current operational network of 51 nodes in the shape of a ring, formed by an aggregation ring and other access rings. Whereas T2 defines a trend in future RAN design with a hierarchical tree structure, presenting two aggregation stages and other access stages. As suggested by the PASSION project, we limit T2 to 128 nodes. Fig. 5 illustrates the two RAN topologies employed in this evaluation. In both topologies, the transport nodes are classified into four types (AG1,

AG2, AC1, and AC2*), as described and illustrated in the figure. On the one hand, this classification helps on having flexibility in the choice of parameters (i.e., the values of the characteristics) for each topology and scenario. On the other hand, the number of parameters is small (i.e., only four) in comparison to the number of transport nodes, e.g., 51 in the smallest topology.

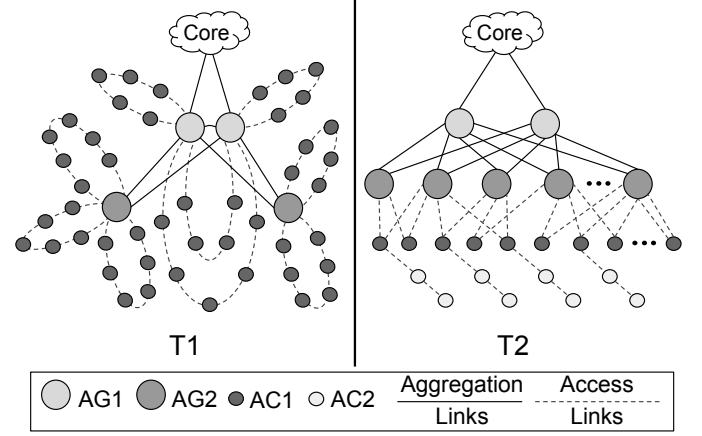


Fig. 5. Types of evaluated RAN topology.

Computing Resources. We focused on the processing capacity (i.e., CPU) because this metric has been the most common bottleneck for the computing devices in the context of network planning and vRAN optimization [25], [26]. CR values in Table 2 indicate the number of CPUs or a range in the case of RC scenario. In this RC scenario, a specific value is random selected (inside the range) when generating input data. The CRs capacity was designed taking into consideration the CPU utilization profile of the RAN software from OpenAirInterface (OAI), as shown in Table 3. The exact values may vary according to the adopted software components and computing device, but similar profiles have been reported in different works.

Bandwidth. The link capability considers the 5G-Crosshaul and PASSION projects and their strategies, i.e., current and future networks, respectively. We define the bandwidth following the standards provided by the IEEE Alliance [29]. In this sense, we distinguish the interface capacities between the two network topologies. 5G-Crosshaul uses links capacity from 40 Gbps to 400 Gbps in the aggregation nodes (AG1 and AG2) and 10 Gbps to 40 Gbps in the access nodes (AC1 and AC2). PASSION Project (future network) operates from 100 Gbps to 1 Tbps in the aggregation nodes and from 40 Gbps to 100 Gbps in the access nodes.

Latency. To reach the latency inputs, we considered four components. (i) Computing latency refers to the time consumed in the forwarding process. (ii) Fiber latency is related to propagation delay in optical fibers. (iii) The Optic is the delay of the optical device without electronic processing. (iv) The regenerator transforms the optical signal into electric signals. Based on these four components, we employed two strategies, one for each topology. In the first strategy, T1 uses only the Computing and Fiber components. However, all link distances in T1 are available, so the propagation

*There is no AC2 in the T1 topology due to the rings.

TABLE 2
Scenarios employed in the evaluation.

Scenarios		Low Capacity (LC)				Random Capacity (RC)				High Capacity (HC)			
Transport Nodes		AG1	AG2	AC1	AC2	AG1	AG2	AC1	AC2	AG1	AG2	AC1	AC2
Computing Resources	†	16	16	8	8	16	16	8	8	32	32	16	16
	‡					32	32	16	16				
	‡					16	16	8	8	64	64	32	32
Bandwidth (Gbps)	†	100	40	25	10	100	40	25	10	400	100	40	25
	‡	800	100	50	40	400	100	40	25				
	‡					1000	400	100	50	1000	400	100	50
Latency (ms)	Computing	†, ‡	0.002				0.05-0.002				0.05		
	Fiber	†, ‡	0.000005				0.000005				0.000005		
	Optic	‡	0.010625				0.010625				0.010625		
	Regenerator	‡	0.0005				0.0005				0.0005		
RU Nodes		†, ‡	-				F1 and R1				-		

TABLE 3
RAN Protocol Stack CPU Utilization [26]–[28].

RAN Protocol	CPU Utilization (cores)
RRC	0.49
PDCP	0.49
High RLC	0.0245
Low RLC	0.0245
High MAC	0.343
Low MAC	0.343
High PHY	0.833
Low PHY	2.352
Total	4.9

delay is directly computed by the distance versus delay propagation. In the second strategy, T2 cannot directly compute the propagation delay, although all components are considered. In this case, the PASSION project performed a study that derived statistical information about potential topologies minimum, average, and maximum link distance and the number of hops. Therefore, the link distance is developed with minimum data for HC scenario, average, and maximum for LC scenario, and all of them for RC scenario [30].

RU Nodes. To evaluate the scenarios (and topologies) with different demands, we considered two configurations for the number of RU nodes connected to the transport nodes: F1 (Fixed 1) – exactly one RU node is connected to each transport node and R1 (Random 1) – zero or one (randomly chosen during input data generation) RU node is connected to each transport node. However, no RU node is connected to any AG1 in any topology scenario, as recommended by 5G-Crosshaul [31] and PASSION [32] projects.

Table 4 summarizes the parameters of the functional splits employed in the evaluation. The priority of each DRC (used in the third stage of the PlaceRAN model) follows the O-RAN Alliance specifications [23]. According to the split options, the maximum tolerated latency is defined for each RAN sub-path: backhaul (Core-CU), midhaul (CU-DU), and fronthaul (DU-RU). Moreover, according to the split options, the minimum acceptable bandwidth is defined for each RAN sub-path. However, we adopted different RF devices for T1 and T2 topologies, which implied in different bandwidths for each network, as shown in Table 4. In T1, we assumed the RF devices have the following characteristics: 40 MHz bandwidth, 32 antenna ports, 8 MIMO layers, 216

Physical Resource Blocks (PRBs), and 15 kHz subcarrier spacing per macro BS [33]. In T2, we assumed the RF devices have the following characteristics: 100 MHz bandwidth, 32 antenna ports, 8 MIMO layers, 132 PRBs, and 60 kHz subcarrier spacing per macro BS [33].

We run all experiments in a Virtual Machine (VM) with Ubuntu 18.04, 16 vCPUs, 1 TB RAM, and 40 GB of the virtual disk. The VM is hosted in a server DELL PowerEdge M620 with two Intel Xeon E5-2650 @ 2 GHz. We used Python 2.7.17 and docplex 2.4.61 for implementing the PlaceRAN model, and the solver used was IBM CPLEX 12.8.0. The source code and the input data used in the evaluation is publicly available on Github*.

4.2 Results

We organize the evaluation of the PlaceRAN model into four parts as described in the following. The first part of the evaluation examines the correlation between the minimization of CRs and the maximization of the aggregation level. The second part presents details about the DRC choices made by PlaceRAN. The third part investigates the aggregation process in more detail, mainly how computing and network resources impact this process. The fourth part of the evaluation confirms the relevance of the three stages of PlaceRAN. In this part, we also evaluate the impact of the number of paths while employing k-shortest paths. Finally, we summarize our main observations of these four parts of the evaluation in the end the section.

CRs and Aggregation level

According to Equation 1, the primary objective of PlaceRAN is finding the best trade-off between the minimum amount of CRs (Φ_1) and the maximum amount of grouped RAN VNFs, i.e., the aggregation level (Φ_2). In order to make them comparable, we normalized the amount of CRs and the aggregation level in a percentage scale. The percentage of used CRs corresponds to the ratio of CRs running any positive number of virtualized functions from the set $\mathcal{F}' = \{f_2, f_3, f_4, f_5, f_6, f_7, f_8\}$. In order to compute the percentage of aggregation level, we assume that the highest achievable value of Φ_2 is given by $|\mathcal{F}'| \times |\mathcal{B}|$, which represents all virtualized functions running in a single CR.

*<https://github.com/LABORA-INF-UFG/NG-RAN-model>

TABLE 4
Parameters of the functional splits.

DRC		Split Options		Tolerated latency - one way (ms)			5G-Crosshaul bandwidth (Gbps)			PASSION bandwidth (Gbps)		
N ^o	Priority	High	Low	Core-CU	CU-DU	DU-RU	Core-CU	CU-DU	DU-RU	Core-CU	CU-DU	DU-RU
1	4	O1	O7	1.5~10	1.5~10	0.250	2.97	5.4	17.4	9.9	13.2	42.6
2	1	O2	O7	1.5~10	1.5~10	0.250	2.97	5.4	17.4	9.9	13.2	42.6
7	6	O1	O6	1.5~10	1.5~10	0.250	2.97	5.4	5.6	9.9	13.2	13.6
8	5	O2	O6	1.5~10	1.5~10	0.250	2.97	5.4	5.6	9.9	13.2	13.6
12	10	O1	-	1.5~10	1.5~10	-	2.97	5.4	-	9.9	13.2	-
13	9	O2	-	1.5~10	1.5~10	-	2.97	5.4	-	9.9	13.2	-
17	8	-	O6	1.5~10	-	0.250	2.97	-	5.6	9.9	-	13.6
18	7	-	O7	1.5~10	-	0.250	2.97	-	17.4	9.9	-	42.6
19	25	-	-	1.5~10	-	-	2.97	-	-	9.9	-	-

Fig. 6 shows the percentage of used CRs (X-axis) and the percentage of aggregation level (Y-axis) of each solution obtained in three scenarios (LC, RC, and HC) and in two configurations of RU nodes (F1 and R1). As expected, as capacity increases there is a trend in increasing the aggregation level and decreasing the used CRs. However, the RAN topology has a significant impact on the solutions. T1 topology, which represents the present RAN topology, tends to limit the benefits of increasing the resources. For example, while comparing the low amount of resources (LC) with the intermediary amount of resources (RC), the configuration F1 exhibits improvement in aggregation level but not in the number of used CRs. Additionally, the hierarchical topology adopted by T2 is robust to the configurations of RU nodes, i.e., to the demand, mainly as the amount of resources increases. In general, the modern T2 topology also presents better solutions in both aspects, percentage of aggregation level and percentage of used CRs.

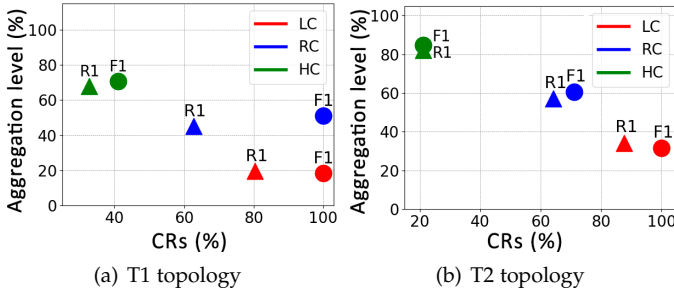


Fig. 6. The relation between aggregation level and number of used CRs.

Fig. 6 represents the first stage of the PlaceRAN model and the consequent totality of aggregation levels. For a more detailed study, we show Table 5 considering the results of the Transport Nodes (AG1, AG2, and AC1) aggregation level and the CRs usage. However, we analyzed only the T1 topology because this network presents non-homogeneous behavior compared with the T2 topology. In this context, we did not consider the AC2 type of Transport Nodes because this does not found in T1 topology. Based on Table 5, we can observe that AG1 concentrates aggregations of the virtualized functions of 92.3% for the HC scenario with the F1 for RU Nodes and 79.6% for R1. Moreover, it aggregated in the AG2 nodes only one CR using R1 and two CRs with F1, further than AC1 did not present any aggregation level. In this sense, it aligned with the model objectives of concentrating VNFs near the core network. For the RC

scenario, aggregations were less than 60% in AG1, and especially for the Transport Nodes type F1 reached 30.8% in AC1. Finally, we observed a high level of aggregation in AC1, with 62.8% and 81.6% for the Transport Nodes R1 and F1 in the LC scenario. For the LC and RC scenarios, we observe an increased use of CRs in AC1 nodes, which results in low aggregation of RAN's VNFs.

TABLE 5
Aggregation level of the T1 topology

		LC		RC		HC	
		R1	F1	R1	F1	R1	F1
AG1	*	26.7	18.4	58.9	51	92.3	79.6
	#	2	2	2	2	2	2
AG2	*	10.5	0	10.3	30.6	7.7	20.4
	#	1	0	1	2	1	2
AC1	*	62.8	81.6	30.8	18.4	0	0
	#	12	20	4	7	0	0

* Aggregation level (%); # Number of CRs

DRCs options

This study analyzes the DRCs chosen by the PlaceRAN model. Fig. 7 shows the amount and options of DRCs in three scenarios (LC, RC, and HC) with the two RU Nodes (F1 and R1) for both investigated topologies. We join the nine DRCs from the five architectures shown in Fig. 1 in four groups for a precise analysis. In this context, we group the four DRCs (DRC1, DRC2, DRC7, and DRC8), named NG-RAN (3), from 3 Independent Nodes architectures (O-RAN Low Split and SCF Low Split). We called NG-RAN (2) for DRC12 and DRC13 from the RU and DU integration architecture. Moreover, we consider DRC17 and DRC18 in the C-RAN architecture and DRC19 in the D-RAN architecture. Furthermore, the shade of their respective color is according to the determined weights DRCs defined on the third stage of the PlaceRAN model. In this case, the choice of the best DCRs set is associated with the latency and bandwidth restrictions imposed by the network and the CRs available.

The first observation concerns the total number of DRCs assessed by each scenario, given the difference of the topologies and strategies between RU Nodes R1 and F1. In this sense, Fig. 7(a) presents the T1 topology with 39 DRCs for R1 and 49 DRCs for F1. Moreover, Fig. 7(b) shows 101 DRCs for R1 and 126 DRCs for F1 in the T2 topology. Observing the DRCs result's behavior, Fig. 7 shows that the PlaceRAN model applied a distinct number of DRCs types

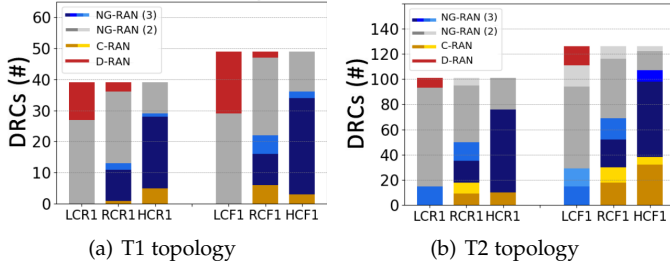


Fig. 7. DRCs chosen on the three scenarios

for each scenario. For example, the model defined two types of DRCs for the LC scenario with RU Nodes F1 for the T1 topology and five DRCs types for the same scenario in the T2 topology. The DRC types increase is expected because of two main factors: (i) maximization of aggregation and (ii) crosshaul restrictions. For the first, the model's priority is to aggregate the maximum of VNFs following the DRCs weight of Table 2. Moreover, the model did not prioritize the reduction of the number of DRCs types. For the second factor, the crosshaul restriction limited the range of the number of DRCs types chosen due to the crosshaul link capacity (bandwidth and latency). It is worth mentioning that the CRs capacity applied not presented restriction for any scenarios.

Another significant analysis is the choice of DRCs according to the architectures defined. For example, the PlaceRAN model did not define D-RAN for thw HC scenario in both topologies. However, D-RAN has high relevance in the T1 topology with the LC scenario, mainly in the LC scenario with RU Node F1, reaching 40.8% (#20). This behavior is directly related to the crosshaul capacity restriction and more significant in the T1 topology due to the ring format. In this case, the capacity of the AC1 links was shared with several nodes. Moreover, observing the two DRCs of the C-RAN architecture, we can see that the PlaceRAN model suggested a number greater of DRCs for the HC scenario in both topologies and with the two RU Nodes. Furthermore, the model did not achieve any C-RAN DRC in the LC scenario instead of the HC scenario. This behavior occurs because the C-RAN architecture maximizes the vCU function's centralization, and in this case, it is required more crosshaul capacity.

DRCs of the NG-RAN(2) architecture demand less network capacity. Therefore, these DRCs are widely picked up in the LC scenario and rarely chosen in the HC scenario. For example, the model reached 77.2% (#78) in the LC scenario with RU Nodes R1 and only 15% (#19) in the HC scenario with F1 for the T2 topology. The solution founded by the PlaceRAN model for DRCs NG-RAN(2) was the best option for the strict crosshaul capacity because the functional split has a high tolerance of latency and low capacity compared with a functional split DU-RU presented in Table 2. Finally, the NG-RAN(3) architecture, although the most relevant DRC type weight in the third stage and follows the O-RAN initiatives, is not entirely feasible because of the crosshaul capacity. However, the model reached expressive results in the HC scenario, reaching 61.6% (#24) with RU Nodes R1 and 67.4% (#33) for R1 in the T1 topology. Furthermore, the

model achieved 65.4% (#66) for RU Nodes R1 and 54.8% (#67) F1 for the T2 topology. Otherwise, the NG-RAN(3) architecture is not feasible for the LC scenario in the T1 topology, as in previous analyses due to the restrictions imposed by the crosshaul aligned the characteristic of high distribution in reason of the three radio nodes.

Network Resources Impact

This analysis investigates the correlation between the three stages of the PlaceRAN model and the network resources occupation. Based on the two previous analyses, we observe that the crosshaul was the main restriction for the PlaceRAN model. In this sense, we chose the T1 topology to highlight the constraints of this topology in the design of fifth-generation networks. Therefore, we selected ten characteristics for investigating this correlation for the three scenarios (LC, RC, and HC), with the two RU Nodes, as shown in Fig. 8. We organize these characteristics into two types since they are associated with the model and the network capacity. The characteristics based on the PlaceRAN model are indicated with a red marker (aggregation level, DRCs usage, and DRCs weight). The network capacity is associated with Transport Nodes' characteristics (AC1 link, AC1 CRs, AG2 link, AG2 CRs, AG1 link, AG1 CRs, and latency), and we mark it in blue in Fig. 8.

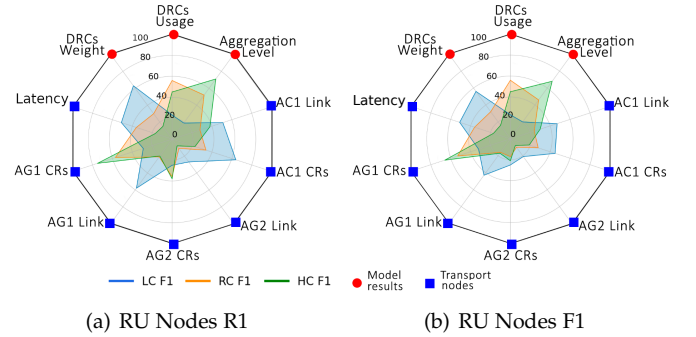


Fig. 8. Model stages versus network resources evaluation.

Observing the characteristics of the PlaceRAN model, the RU Nodes R1 in Fig. 8(a) and F1 in Fig. 8(b) show similar results for the three scenarios. The aggregation level presented the same evaluating in the HC scenario, upper than 60% and lower than 20% in the LC scenario. The DRCs usage showed the number of DRCs types in percent unit (nine DRCs equals 100%). The PlaceRAN model applied almost 60% of total DRCs types in the RC scenario and around 20% in the LC scenario. In this case, we can see the appropriate aggregation level for the HC scenario and high DRCs usage for the RC scenario. Moreover, we can observe the DRCs weight, which is the sum result of DRCs chosen priority detailed in Table 2. This characteristic shows which smaller outcome represents the best solution. Consequently, the HC scenario reached an effect lower of 20% with the best solution. This behavior was the opposite for the LC scenario, with results around 60%. These results are connected directly with the network capacity, presented in the following.

The characteristics of Transport Nodes consumption, CRs, links, and latency are analyzing together because

the behavior is complementary. These characteristics show that the HC scenario had the highest occupation of RCs under AG1 nodes, obtaining close to 70% for RU Nodes R1 and 80% F1. Moreover, the latency average presented a difference significant between the LC scenario and the HC scenario. For example, we observed a variation of approximately 45% for the RU Nodes R1 and 38% for F1. Considering absolute values, it is upper 5ms in the LC scenario, contributing directly to the low performance in this scenario. For instance, the requirement of DU-RU was 0.250ms, as presented in Table 2.

The HC scenarios' link capacity did not reach more than 25% of occupation, resulting in a high aggregation of VNFs showed by the aggregation level. The LC scenario presented a high AC1 CRs and the link occupation, compared with the HC scenario because this topology has links that support low capacity. This behavior happens on the AG1 link occupation, for example, almost 60% of occupation, and the high delay average. It is resulting in a low aggregation level and the DRCs usage with high DRCs weight. However, the AG2 link did not present a significant consumption variation for the scenarios. This behavior occurs since the T1 topology has a particular characteristic, where AG1 nodes concentrate all 51 nodes and AG2 nodes only part of these nodes.

Three stages of PlaceRAN model and k -paths

In this last analysis, we investigate the PlaceRAN model from two perspectives. First, we study the importance and behavior of the three stages of the model. After, we observe the relation of K -paths with solutions found by the PlaceRAN model. The second and third stages of the PlaceRAN model deal with tie cases and define which solution is better. In this sense, Table 6 shows an example of a real case with the RC scenario for RU Nodes F1 in the T1 topology. The solutions found by the second and third stages presents significant improvements to the final solution. Therefore, Table 6 shows the nine DRCs configurations chosen with the solutions found by three stages. The first stage defined the maximum aggregation level and minimum number of CRs operating in this scenario. The second stage found the smallest number of DRCs that obtain the aggregation level, achieved in the first stage. It is fundamental to observe that the number of DRCs used in the second stage dropped from eight to five. Finally, the third stage defined the picks of DRCs according to the weights, which in this article, we prioritize the O-RAN solution. In this case, we can observe the number of DRC19 (D-RAN) decreases significantly, from 12.3% to 4.1%, given that D-RAN has low priority (weight) in O-RAN.

Finally, we analyze the PlaceRAN model results for different amounts of K -paths from the core to each RU Nodes spread across the topology. In some cases, PlaceRAN did not find an optimal solution but a possible and viable solution, e.g., in some configurations with the T1 topology. Therefore, we calculated the objective function gap (%) between this possible solution and the optimal one. For example, Fig. 9 shows k -paths for the three scenarios with RU Nodes F1 in the T1 topology. The x -axis represents the variation of k -paths between $(1 \leq k \leq 6)$ since Moreover, the y -axis depicts three views: (i) the objective function value in the top, (ii) the amount of CRs used by the model in the middle,

TABLE 6
Analyzing the three stages of the PlaceRAN model.

DRCs	Stage 1	Stage 2	Stage 3
1 - NG-RAN(3)	2%	0%	0%
2 - NG-RAN(3)	14.3%	22.4%	20.5%
7 - NG-RAN(3)	0%	0%	0%
8 - NG-RAN(3)	6.1%	10.2%	12.2%
12 - NG-RAN(2)	2%	0%	0%
13 - NG-RAN(2)	40.9%	42.9%	51%
17 - C-RAN	8.2%	0%	0%
18 - C-RAN	12.2%	12.2%	12.2%
19 - D-RAN	14.3%	12.3%	4.1%
Total	100%	100%	100%

and (iii) the aggregation level achieved by the solution in the bottom bars.

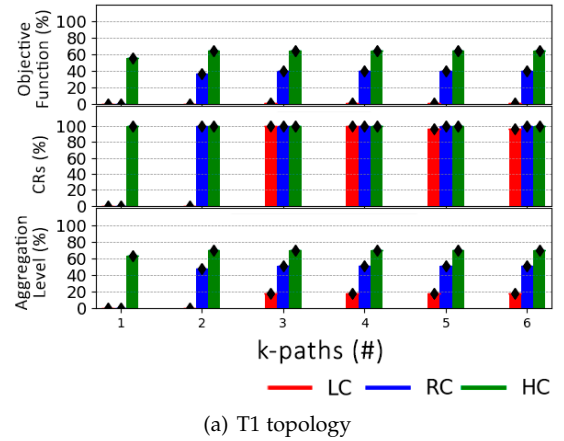


Fig. 9. K-shortest paths for the T1 topology.

We can observe that the PlaceRAN model reached a possible objective function near 60%, using 100% of CRs, and above 60% of aggregation level with $k = 1$ for the HC scenario. In the same analysis, the model found the objective function near 40% for the RC scenario with $K = 2$, also using 100% of CRs and 50% of the aggregation level. We can see that the objective function, CRs, and aggregation level stabilized for $k \geq 3$. This stabilization means that for $k > 3$, the model's solutions did not present significant variations for the T1 topology because $k > 3$ increases the problem's complexity by adding redundant paths in the topology. It is important to highlight that the same behavior occurs for the T2 topology.

Discussion

This section discusses the PlaceRAN model results based on the fourth analysis with a global view aiming to correlate the model's characteristics. Achieving the model's objective is necessary to overcome the crosshaul constraints for the best placement of RAN's VNFs to maximize the aggregation level, minimize the CRs, decide to the lower DRCs numbers, and prioritize the DRC choices based on strategies. In this sense, the solution takes the placement best decision focused on overcoming the crosshaul limitations. However, the constraint did not restrict the D-RAN architecture picked up in some scenarios, limiting the fifth-generation network's deployment. The PlaceRAN model reached a high aggregation

level for scenarios without crosshaul restriction resources, e.g., in the two AG1 CRs, centralizing the high RAN's VNFs and leverage the fifth-generation networks based on O-RAN initiatives. Moreover, the PlaceRAN model found the best optimize of k -paths possible considering the crosshaul characteristics.

The behavior of the position of CU nodes and their aggregation in the Transport Nodes (mainly in AG1 nodes) has significant importance for RAN development. For NG-RAN(3) architecture, the aggregation CU nodes VNFs are all in the AG1 nodes for both topologies, less for the LC scenario of the T1 topology, which does not have NG-RAN (3) DRCs types. This aggregation level presented as the best option of deploy the vNG-RAN. However, the C-RAN architecture did not have the same performance once it achieves 100% of CU nodes VNFs in the HC scenario in the AG1 nodes and 100% of CU nodes VNFs in the LC scenario in the AC1 nodes for the T1 topology. In this case, the aggregation in the AC1 nodes did not contribute to the CU centralization. The NG-RAN(2) result presented a spread aggregation of CU nodes in the different scenarios but reaches 0% of CU node position in the AC1 for any scenarios of the T2 topology and only 0% for the HC scenario in the T1 topology. Moreover, D-RAN did not have this behavior due to the monolithic architecture.

Finally, although the work does not explore the costs issue, the three scenarios chosen are directly oriented to investment. For example, for the HC scenario with the best solution performance, there is a greater need for resources on the network and consequently high investment. Moreover, the topologies analyzed show that the structure influences the results. For instance, the T1 topology is not fitted to the fifth generation networks' evolution, mainly because of total latency considering several computational processing of the routing devices in the AC1 layer. Furthermore, we analyze the T1 topology with an intermediate RAN channel with 40MHz, different from the 100MHz forecasted. Therefore, our analysis shows the need to redesign the network and the investment for the T1 topology. In the same way, the T2 topology also needs investment, mainly because of the optical devices for the crosshaul. Moreover, the project analyzed (5G-crosshaul and PASSION) show an imbalance between the occupation of resources. For example, in the HC scenario, AC1 nodes, and AC2 nodes presented a low occupation in links and CRs, which can be optimized, consequently reducing investment.

5 RELATED WORK

Recently, RAN has faced an intense process of *softwarization* and virtualization, which has driven into a fast evolution. However, this scenario also created a misalignment of several works related to the (virtual) network function placement due to the raise of multiple initiatives in a short period of time. These initiatives are usually led by the standard developer organizations, e.g., 3GPP, ITU-T, and ETSI. Moreover, the O-RAN alliance drives some directions, such as vNG-RAN focusing on the disaggregation of radio functions for network efficiency and performance. In this context, Table 7 shows several relevant works regarding

Optimization Goals and Disaggregated RAN, considering the type of the nodes modeled and the number of DRCs.

Optimization Goals. This characteristic is the most relevant when comparing the related work since investigations with different optimization goals have distinct problem formulations, achieve different results, and, commonly, drive to diverse insights. In some works, the focus is to maximize the number of VNFs running in a single CU. For example, for Garcia-Saavedra et al., the CU is co-located with the core, and D-RAN is not an option. However, for Fonseca, Correa, and Cardoso [15], D-RAN is taken into consideration, and different positions are evaluated for CU. The maximization of CU and BBU nodes are aimed at in several investigations [14], [15], [34], [35], [40]. In C-RAN architecture, the fronthaul latency and the capacity of data rate links are widely analyzed [12], [16], [17], [19], [37], [40]. Based on RAN centralization, Song et al. [18] and Matoussi et al. [37], focus on the CRs efficiency. Furthermore, the RAN transformation is targeted into maximization of centralization, the CRs efficiency, and crosshaul link costs assessment by Arouk et al. [38] and Masoudi, Lisi, and Cavdar [39].

Murti et al., in their initial work [12] and in its extended version [13], have the closest investigation to ours. These authors are also approaching the problem of finding the best trade-off between the minimum number of CRs and maximum aggregation level. However, they consider only vCUs, while DUs are fixed and close to (RU)s, i.e., provided as input. In our work, we consider not only vCUs, but also vDUs, making our problem more general. We formulated the problem as a Nonlinear Programming model, with binary variables, linear constraints, and a nonlinear objective function (from the first stage). We were able to create an equivalent representation of the nonlinear objective function using Min and Max functions. Therefore, our model can be solved exactly by a *conventional* solver, e.g., the IBM CPLEX.

Disaggregated RAN. The number of types of the RAN nodes and the number of DRCs are related to the flexibility and complexity of the problem under investigation. The types of the RAN nodes available and the number of DRCs represented are related to the accuracy of describing the real-world disaggregated RANs. In this context, our model represents all types of the RAN nodes and all industry DRCs, i.e., our model describes precisely the present disaggregated RANs. Additionally, our model is ready for supporting other DRCs by just changing the set \mathcal{D} .

During the classification of the related work in terms of RAN nodes and number of DRCs, we adopted a conservative approach. Therefore, most of the related work had its benefits amplified for the disaggregated RAN, e.g., Murti et al. [12], [13] describe CU, DU, and RU in the system model, but the paths between from RU are not taken into account. This happens because each RU has only a single link connecting to a single DU. Therefore, our model is again more general than the state-of-the-art.

Given the complexity of the VNF placement problem, several works in the literature adopt an approximate and heuristic approach [17], [19], [34], [36], [37], [40]. As expected, in general, the main advantage of this type of approach is the reduced computing cost and the main drawback is the suboptimal solutions. As discussed in [13], suboptimal vRAN solutions have large cost impact in the

TABLE 7
Related work.

Works	Optimization Goals	Disaggregated RAN	
		Nodes	DRCs
[14]	Maximization of CU centralization and evaluation of Latency Edge	CU-RU	3
[15]	Maximization of CU centralization and flexible CU positioning	CU-RU	5
[34]	Maximization of BBU centralization and minimize the overall latency	BBU-RRH	1
[17]	Dynamic CU and wireless fronthaul to minimize the energy	CU-DU	4
[19]	Minimize the cost of VNF chain on substrate network	BBU-RRH	1
[35]	Identify the ideal position of the centroid for the BBU	BBU-RRH	1
[36]	Maximize DU distribution under non-dedicated optical network	CU-DU	2
[37]	Minimize the CRs and fronthaul bandwidth	BBU-RRH	3
[18]	Minimize the computational costs	Monolithic	1
[38]	Minimize the CRs and overall routing costs	CU-DU-RU	1
[39]	Minimize the total cost of ownership by DU pool	DU-RU	4
[16]	Minimize the nodes and latency; maximize the data rate	CU-DU-RU	2
[40]	Minimize interference and fronthaul links to optimize the network	CU-DU	4
[12], [13]	Minimize the vRAN cost and overall routing, based on CU's positioning	CU-DU-(RU)	3
PlaceRAN	Minimize CRs and maximize vNG-RAN's radio functions aggregation	CU-DU-RU	9

long-tem. Additionally, our strategy has advantages in comparison with approximate and heuristic approaches. First, PlaceRAN is able to obtain the optimal solution in satisfactory time for several real-world networks, mainly for the most modern topologies. Second, when the computation is interrupted before achieving the optimum, we know the gap of the suboptimal solution obtained by PlaceRAN.

6 FINAL REMARKS

In this work, we address the optimization problem of vNG-RAN placement, which is still a paradigm for standardization and industry and relevant for deploying the fifth-generation RAN with the PlaceRAN solution. In this sense, we developed an optimal optimization solution to deliver the best possibility of allocating RAN's VNFs to reduce the use of computational resources and reach maximum aggregation and consequent centralization of RAN's protocols and units. In addition to overcoming the limitations of crosshaul networks by choosing the best path. We developed the concept of DRC disaggregation combinations, reduced the number of DRCs in the network, and inserted the strategy concept for choosing DRCs. All this in scenarios and environments of real networks and with the possibility of implementation in any vNG-RAN.

For future work, we envision advances in the solution concerning the time factor. In the scope of choosing the best path for crosshaul networks, we will evolve the solution to deal with traffic in the flow format, avoiding, even more, the waste of bandwidth. In computing resources, our strategy is to be even more aligned with O-RAN initiatives. Therefore, we will be introducing the type of processing to be defined for each virtualized radio function, for example, general-purpose processor (GPP) or specific purpose processor (SPP).

ACKNOWLEDGMENT

This work was conducted with partial financial support from the National Council for Scientific and Technological Development (CNPq) under grant number 130555/2019-3 and from the Coordination for the Improvement of Higher Education Personnel (CAPES) - Finance Code 001, Brazil.

REFERENCES

- [1] 3GPP, "System Architecture for the 5G (Release 15)," Technical Recommendation 23.501, 2018.
- [2] G.-T. ITU-T, "Transport network support of IMT-2020/5G," 2018.
- [3] T. ETSI, 5G; NG-RAN; *Architecture description (ETSI TS 138 401 V15.5.0 (2019-05))*, 2019.
- [4] L. Gavrilovska, V. Rakovic, and D. Denkovski, "From Cloud RAN to Open RAN," *Wireless Personal Communications*, pp. 1–17, 2020.
- [5] P. Marsch *et al.*, *5G system design: architectural and functional considerations and long term research*. John Wiley & Sons, 2018.
- [6] R. Agrawal *et al.*, "Cloud RAN challenges and solutions," *Annals of Telecommunications*, vol. 72, no. 7-8, pp. 387–400, 2017.
- [7] C. Badulescu and J. Triay, "ETSI NFV, the Pillar for Cloud Ready ICT Deployments," *Journal of ICT Standardization*, vol. 7, no. 2, pp. 141–156, 2019.
- [8] C. J. Bernardos *et al.*, "Network virtualization research challenges," IETF, Tech. Rep., 2019.
- [9] P. Sehier *et al.*, "Transport Evolution for the RAN of the Future," *Journal of Optical Communications and Networking*, vol. 11, no. 4, pp. B97–B108, 2019.
- [10] M. Masdari *et al.*, "An overview of virtual machine placement schemes in cloud computing," *Journal of Network and Computer Applications*, vol. 66, pp. 106–127, 2016.
- [11] A. Laghrissi and T. Taleb, "A survey on the placement of virtual resources and virtual network functions," *IEEE Communications Surveys & Tutorials*, vol. 21, no. 2, pp. 1409–1434, 2018.
- [12] F. W. Murti *et al.*, "On the Optimization of Multi-Cloud Virtualized Radio Access Networks," *arXiv preprint arXiv:2002.10681*, 2020.
- [13] F. W. Murti *et al.*, "Optimal Deployment Framework for Multi-Cloud Virtualized Radio Access Networks," *IEEE Transactions on Wireless Communications*, pp. 1–1, 2020.
- [14] A. Garcia-Saavedra *et al.*, "Fluidran: Optimized vRAN/MEC orchestration," in *IEEE INFOCOM Conference on Computer Communications*, 2018, pp. 2366–2374.
- [15] F. Fonseca, S. Correa, and K. Cardoso, "Optimizing allocation and positioning in a disaggregated radio access network aware of paths through the core infrastructure," in *Anais do XXXVII Simpósio Brasileiro de Redes de Computadores e Sistemas Distribuídos*, 2019, pp. 791–804.
- [16] J. Yusupov *et al.*, "Multi-objective function splitting and placement of network slices in 5G mobile networks," in *IEEE Conference on Standards for Communications and Networking (CSCN)*, 2018, pp. 1–6.
- [17] D. Harutyunyan *et al.*, "CU placement over a reconfigurable wireless fronthaul in 5G networks with functional splits," *International Journal of Network Management*, vol. 30, no. 1, p. e2086, 2020.
- [18] S. Song *et al.*, "Clustered virtualized network functions resource allocation based on context-aware grouping in 5G edge networks," *IEEE Transactions on Mobile Computing*, vol. 19, no. 5, pp. 1072–1083, 2019.
- [19] O. Arouk *et al.*, "Multi-objective placement of virtual network function chains in 5G," in *IEEE 6th International Conference on Cloud Networking (CloudNet)*, 2017, pp. 1–6.

- [20] L. M. P. Larsen, A. Checko, and H. L. Christiansen, "A Survey of the Functional Splits Proposed for 5G Mobile Crosshaul Networks," *IEEE Communications Surveys & Tutorials*, vol. 21, no. 1, pp. 146–172, 2019.
- [21] 3GPP, "Study on New Radio Access Technology; Radio Access Architecture and Interfaces (Release 14)," 3rd Generation Partnership Project (3GPP), Technical Recommendation (TR) 38.801, 2017.
- [22] Mavenir, "Transforming the Radio Access Network - Mavenir's Virtualized RAN," Mavenir, Tech. Rep., 2019.
- [23] O. R. Alliance, "Cloud Architecture and Deployment Scenarios for O-RAN Virtualized RAN," *White Paper*, 2020.
- [24] 3GPP-TR21.916, "System Architecture for the 5G (Release 16)," Technical Recommendation 21.916, 2020.
- [25] P.-C. Lin and S.-L. Huang, "Performance profiling of cloud radio access networks using openairinterface," in *Asia-Pacific Signal and Information Processing Association Annual Summit and Conference (APSIPA ASC)*, 2018, pp. 454–458.
- [26] Y. Hu and J. Wang, "Architectural and Cost Implications of the 5G Edge NFV Systems," in *IEEE 37th International Conference on Computer Design (ICCD)*, 2019, pp. 594–603.
- [27] C. Y. Yeoh *et al.*, "Performance study of LTE experimental testbed using OpenAirInterface," in *18th International Conference on Advanced Communication Technology (ICACT)*, 2016, pp. 617–622.
- [28] K. Kazunari, "Approach to Commercial Use of OAI," available at <https://www.openairinterface.org/docs/.../20171108.pdf>(accessionNovember11,2020).
- [29] J. D'Ambrosia, "The State of Ethernet," 2017.
- [30] Huawei, "White Paper on Huawei MS-OTN Low-latency Network solution," available at <https://www-file.huawei.com/.../huawei-optical-network-low-Latency-solution-white-paper-en.pdf>(accessionNovember11,2020).
- [31] 5G-crosshaul Project, "5G-crosshaul, D1.2: final 5G-crosshaul system design and economic analysis," 2017.
- [32] PASSION Project, "Photonic technologies for programmable transmission and switching modular systems based on Scalable Spectrum/space aggregation for future agile high capacity metro Networks," 2020. [Online]. Available: <http://www.passion-project.eu/project/>
- [33] "ThoR - Deliverable D2.1 - Requirements for B5G backhaul/fronthaul," available at <https://thorproject.eu/wp-content/uploads/2018/12/ThoR-D2.1-Requirements-for-B5G-back-fronthaul-NOT-YET-APPROVED.pdf>(accessionNovember11,2020).
- [34] D. Bhamare *et al.*, "Efficient virtual network function placement strategies for cloud radio access networks," *Computer Communications*, vol. 127, pp. 50–60, 2018.
- [35] B. Mahapatra *et al.*, "Optimal Placement of Centralized BBU (C-BBU) for Fronthaul and Backhaul Optimization in Cloud-RAN Network," in *International Conference on Information Technology (ICIT)*, 2017, pp. 107–112.
- [36] N. Molner *et al.*, "Optimization of an integrated fronthaul/backhaul network under path and delay constraints," *Ad Hoc Networks*, vol. 83, pp. 41–54, 2019.
- [37] S. Matoussi *et al.*, "5G RAN: Functional Split Orchestration Optimization," *IEEE Journal on Selected Areas in Communications*, vol. 38, no. 7, pp. 1448–1463, 2020.
- [38] O. Arouk *et al.*, "Cost optimization of cloud-RAN planning and provisioning for 5G networks," in *IEEE International Conference on Communications (ICC)*, 2018, pp. 1–6.
- [39] M. Masoudi, S. S. Lisi, and C. Cavdar, "Cost-Effective Migration Toward Virtualized C-RAN With Scalable Fronthaul Design," *IEEE Systems Journal*, 2020.
- [40] D. Harutyunyan and R. Riggio, "Flex5G: Flexible functional split in 5G networks," *IEEE Transactions on Network and Service Management*, vol. 15, no. 3, pp. 961–975, 2018.